ACS Partner Journal

Journal of the American Society for Mass Spectrometry

pubs.acs.org/jasms

Article

Oxidized and Reduced Dimeric Protein Complexes Illustrate Contrasting CID and SID Charge Partitioning

Published as part of the Journal of the American Society for Mass Spectrometry virtual special issue "Focus: Ion Chemistry and Electrospray Ionization".

Mengxuan Jia, Yang Song, Chen Du, and Vicki H. Wysocki*

Cite This: https://doi.org/10.1021/jasms.3c00142

Read Online

ACCESS | Metrics & More | Article Recommendations | Supporting Information

ABSTRACT: Charge partitioning during the dissociation of protein complexes in the gas phase is influenced by many factors, such as interfacial interactions, protein flexibility, protein conformation, and dissociation methods. In the present work, two cysteine-containing homodimer proteins, β-lactoglobulin and α-lactalbumin, with the disulfide bonds intact and reduced, were used to gain insight into the charge partitioning behaviors of collision-induced dissociation (CID) and surface-induced dissociation (SID) processes. For these proteins, we find that restructuring dominates with CID and dissociation with symmetric charge partitioning dominates with SID, regardless of whether intramolecular disulfide bonds are oxidized or reduced. CID of the charge-reduced dimeric protein complex leads to a precursor with a slightly smaller collision cross section (CCS), greater stability, and more symmetrically distributed charges than the significantly expanded form produced by CID of the higher charged dimer. Collision-induced unfolding plots demonstrate that the unfolding−restructuring of the protein complexes initiates the charge migration of higher charge-state precursors. Overall, gas collisions reveal the charge-dependent restructuring/unfolding properties of the protein precursor, while surface collisions lead predominantly to more charge-symmetric monomer separation. CID's multiple low-energy collisions sequentially reorganize intra- and intermolecular bonds, while SID's large-step energy jump cleaves intermolecular interfacial bonds in preference to reorganizing intramolecular bonds. The activated population of precursors that have taken on energy without dissociating (populated in CID over a wide range of collision energies, populated in SID for only a narrow distribution of collision energies near the onset of dissociation) is expected to be restructured, regardless of the activation method.

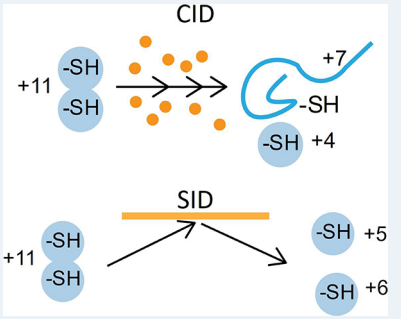

INTRODUCTION

The ability to preserve noncovalent interactions in protein complexes by kinetically trapping solution structures upon transfer into the gas phase, typically by nanoelectrospray ionization (nano-ESI), has enabled native mass spectrometry to emerge as a powerful bioanalytical tool for protein complex analysis.[1−3] The charge state in the gas phase often reflects protein conformation from electrospray,[4,5] and probing the charge-state distribution (CSD) provides clues for protein structural analysis. In addition to the mass measurement of the intact complex, subcomplexes can be generated in the gas phase to provide insights into the stoichiometry and topology/geometry of protein complexes. Two gas-phase dissociation methods for studying quaternary structures of protein complexes by collision with a target are collision-induced dissociation (CID)[6,7] and surface-induced dissociation (SID).[8,9] CID is a multistep process with energy being deposited via a large number of collisions with an inert gas.[10] Typically, CID of protein complexes produces fragments consisting of highly charged monomers and their complementary $(n-1)$-mer products.[7,11] In contrast, during the SID process, the analytes are activated by undergoing a collision with a target surface that is much more massive than either the analyte ion or the collision gases used for CID. SID produces more symmetric CSD of product ions and subcomplexes, providing information on protein topology and connectivity.[12−15] Another useful technique often coupled to native mass spectrometry is ion mobility, which provides rotationally averaged collision cross sections (CCS) of ions in the gas phase and is thus another probe of the gas-phase protein structures.[16,17]

The typical CID process for protein complexes generates asymmetric charge partitioning. Asymmetric charge partitioning during the CID process has been shown to be related to the precursor charge state, internal energy, protein flexibility,

Received: April 20, 2023
Revised: August 1, 2023
Accepted: August 4, 2023

and conformation.[18−22] Jurchen et al. showed that the 15+ α-lactalbumin dimer, which has four intramolecular disulfide bonds in each monomer, dissociates into monomers with a symmetric charge distribution via CID. When the disulfide bonds in the protein were reduced, the charge distribution of the dissociated products become asymmetric, which was explained by the unfolding of the proteins allowed by the increased flexibility gained in the absence of disulfide bonds.[18,19] In addition to flexibility, Hall et al. showed that charge reduction of protein complexes can influence collision-induced modification pathways, as well. The possible pathways include unfolding, noncovalent dissociation, and backbone fragmentation, and the resulting pathway is proposed to be related to the relative energy barriers of each pathway.[22]

In contrast to CID, SID at appropriate collision energies for complexes with structures that are, e.g., not intertwined, is proposed to overcome the high energy barriers of the dissociation pathways and produce subcomplexes with a more symmetric charge-state distribution. Charge-reduced protein complexes have exhibited more "native-like" dissociation patterns in the gas phase based on the collision cross-sections (CCS) of the subcomplexes and on the types of subcomplexes formed.[23]

In this paper, we first focus on the β-lactoglobulin homodimer with disulfide bonds intact (BLG(ox)) and reduced (BLG(red)). We compare the SID patterns of the β-lactoglobulin homodimers with the CID results. Next, we present the influence of the precursor charge state of the reduced and oxidized protein complexes on both the CID and SID pathways. The collision-induced unfolding (CIU) and surface-induced unfolding (SIU) profiles of the precursors at different charge states were also measured to gain insight into the competition between the restructuring and dissociation. In addition, similar experiments on α-lactalbumin were performed to extend the conclusions that can be made for dimeric proteins.

EXPERIMENTAL SECTION

Reagents. Serum amyloid P (SAP) from human serum, avidin, concanavalin A (CONA) from *Canavalia ensiformis*, alcohol dehydrogenase (ADH), β-lactoglobulin (BLG), and α-lactalbumin (ALB) were purchased from MilliporeSigma (St. Louis, MO). All protein complexes were buffer exchanged into 200 mM ammonium acetate (AmAc) (MilliporeSigma, St. Louis, MO) solution using Micro Bio-Spin $P\bar{6}$ columns (Bio-Rad, Hercules, CA). The reduction conditions for disulfide bonds in BLG and ALB were optimized to achieve similar CSD with and without reduction to preserve native-like structures. This milder reduction contrasts with the study by Jurchen et al. in which complete reduction was initiated and reoxidation was prevented by the addition of iodoacetamide; we chose to avoid the restructuring that might be caused by chemical modification. The reduction results were monitored by native MS after online buffer exchange to 200 mM AmAc on a modified Exactive Plus EMR Orbitrap Mass Spectrometer (Thermo Scientific, Walthan, MA). The optimized reduction conditions consist of incubation in 50 mM dithiothreitol (MilliporeSigma, St. Louis, MO) for 20 min at 50 °C for β-lactoglobulin and 0 °C (on ice) for α-lactalbumin. The disulfide-reduced proteins were buffer exchanged into 200 mM AmAc with 5 mM dithiothreitol for measurements on a Synapt G2 instrument (Waters Corporation, Wilmslow, UK). Triethylammonium acetate (TEAA; 20% (v/v) 200 mM; MilliporeSigma, St. Louis, MO) was used for charge reduction.

Instrument Settings. Collision-induced dissociation, surface-induced dissociation, and ion-mobility experiments were performed on a modified Waters Synapt G2 quadrupole/ion mobility/time-of-flight mass spectrometer.[24] Samples were loaded into an in-house pulled glass capillary (Sutter, BF100-78-10), a 0.368 mm diameter platinum wire was inserted into the back of the capillary to provide the spray voltage, and samples were sprayed at complex concentrations of 5−20 μM using nanoelectrospray ionization (nESI). The SYNAPT G2 HDMS (Waters Corporation, Wilmslow, U.K.) is modified with a surface-induced dissociation (SID) device incorporated between a truncated trap traveling wave ion guide and the ion mobility cell.[12] The following instrument parameters were used: sampling cone, 20 V; extraction cone, 2 V; source temperature, 20 °C; trap gas flow, 2 mL/min for MS and SID modes and 4 mL/min for CID mode; trap bias, 45 V. The SID settings are listed in Supplementary Table S1. Collision-induced dissociation (CID) was performed by varying the trap cell collision voltage with the SID set in the transfer mode. Accurate masses were measured on an Exactive Plus EMR Orbitrap instrument (Thermo Scientific) modified with a quadrupole mass filter and a surface-induced dissociation device.[25] The samples were injected on a self-packed buffer exchange column (Bio-Rad $P\bar{6}$ packing material) using an Ultimate 3000 RSLC (Thermo Scientific) coupled to the modified Exactive Plus EMR Orbitrap instrument (Thermo Scientific).[25,26] The mobile phase was 200 mM ammonium acetate. The flow rate was 100 μL/min, and proteins typically eluted within 1.2 min.

CCS Calculation. The theoretical CCS values were calculated from the PDB models of 2Q2M (β-lactoglobulin dimer) and 1BEB (β-lactoglobulin monomer) using the IMPACT software[27] and the projected superposition approximation (PSA) server.[28−31] Based on empirical data, the projection approximation (PA) CCS values need to be corrected by using the equation

$$\Omega' = 1.14 \times \Omega \times \left(\frac{M_{exp}}{M_{pdb}}\right)^{2/3}$$

where Ω′ is the corrected CCS value, Ω is the PA CCS value, M_{exp} is the experimental mass, and M_{pdb} is the theoretical mass calculated from the PDB structure.[22,32] Experimental CCSs were measured following a published protocol[16,33] using cytochrome C (6+, 7+), β-lactoglobulin (7+ to ∼9+), transthyretin (14+ to ∼16+), avidin tetramer (15+ to ∼18+), concanavalin A tetramer (20+, 21+), and serum amyloid P pentamer (22+ to ∼26+) as calibration standards. At the time of this work, no database of CCS values for charge-reduced standards[17] was available. The present paper, however, focuses only on relative CCS changes and not absolute values, so use of corrected PA values after calibration with standards sprayed in ammonium acetate is appropriate.

Data Processing. Data acquired on the Synapt G2 were processed with MassLynx v4.1 and DriftScope v2.1. The drift time profiles were extracted by using TWIMExtract v1.3.[34] The unfolding plots were generated using CIUSuite1.[35] Data acquired on the EMR were processed with an Xcalibur 2.2 (Thermo Scientific). The laboratory frame collision energy is defined as the collision voltage (trap CE for CID and [trap bias −60] for SID) multiplied by the precursor charge state.

https://doi.org/10.1021/jasms.3c00142
J. Am. Soc. Mass Spectrom. XXXX, XXX, XXX−XXX

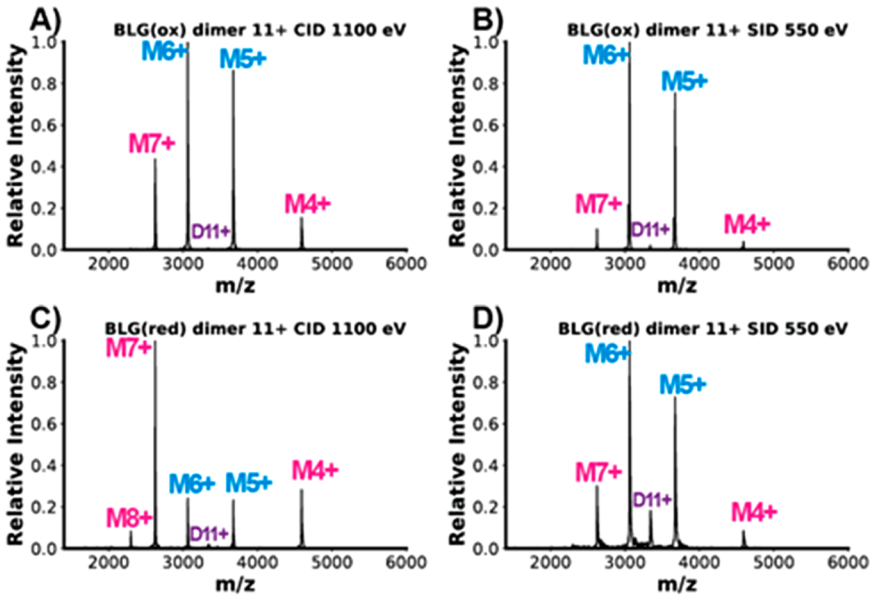

Figure 1. MSMS spectra of the 11+ BLG dimer. (A) CID 1100 eV of BLG dimer with disulfide bonds intact (BLG(ox)); (B) SID 550 eV of BLG(ox) dimer; (C) CID 1100 eV of BLG dimer with disulfide bond reduced (BLG(red)); (D) SID 550 eV of BLG(red) dimer. Blue and pink labels indicate charge symmetrically and asymmetrically distributed monomers, respectively; purple labels indicate precursor peaks, 'M' indicates monomer, 'D' indicates dimer, and the number indicates the charge state.

RESULTS AND DISCUSSION

CID/SID Comparison for Homodimers with Intact vs Reduced Disulfide Bonds. Jurchen et al. previously reported that CID of dimers with intramolecular disulfide bonds within the subunits, such as α-lactalbumin, leads to the generation of almost equally charged monomers while CID of the dimers after reduction of the disulfide bonds results in asymmetrically charged monomers.[18] This change was proposed to be due to the increased flexibility of the proteins after reduction of the *intra*molecular/monomeric disulfide bonds. Hall et al. indicated that low flexibility of a protein subunit would lead to "atypical" CID, leading to symmetric charge partitioning without unfolding.[11] The rigidity effect on SID behavior, previously explored by Harvey et al.[36] without reduction/oxidation of disulfide bonds, was evaluated in the work reported here by dissociating β-lactoglobulin (BLG) dimer and the corresponding partially disulfide-reduced dimer. The dominant charge states of the β-lactoglobulin dimer are from 11+ to 13+ when spraying from 200 mM AmAc (Figure S1A). The gentle reduction conditions used in this work, reduction of an average of one disulfide bond per monomer, do not change the charge-state distribution of the β-lactoglobulin dimer (Figure S1B).

Similarly to the intramolecular disulfide-containing α-lactalbumin previously investigated by the Williams group, native BLG monomers have disulfide bonds although BLG has only two, Cys106−Cys119 and Cys66−Cys160, and one free thiol group at Cys121. Previous research shows that heating will induce aggregation of the BLG which is most likely mediated by the free thiol group.[37] The Cys106, -119, and -121 sit in a very hydrophobic pocket between the α helix and the β sheet of a single monomer. During heating, the unfolding of the monomer causes loss of the helical structure and allows the Cys121 to reversibly create a Cys106−Cys121 disulfide and a free thiol at Cys 119, which induces the aggregation.[38] In order to maintain the interface of the BLG dimer and minimize overall structural change, we optimized the reduction conditions by monitoring the mass shift of the proteins with online buffer exchange native MS.[26,39] We found that in 50 mM dithiothreitol, after 20 min incubation at 50 °C, the average mass increased by 2 Da for each subunit after reduction (Figure S2) which indicates the reduction of only one disulfide bond. Presumably only the water-accessible disulfide bond Cys66−Cys160 has undergone reduction. More monomer was observed in the sample with reduced disulfide bonds (Figure S1B), which suggests that the reduction has an effect on the structure and that it causes a loss of around 30% dimers. Thus, we also compared the CCS of the oxidized 11+ dimer, BLG(ox), and the reduced dimers, BLG(red) (Figure S3), and found there was no significant CCS change after reduction. For each monomer, there is an additional peak corresponding to a mass increase of 324 Da that is due to lactosylation in the samples,[40] and the precursor selection window of ~30 m/z is not narrow enough to exclude all the peaks with the modification.

Native-like dimer with a precursor charge state 11+ and with disulfide bonds intact was selected for dissociation by CID and SID. When CID at 1100 eV is applied, the monomers produced from the 11+ BLG dimer show dominant charge states 6+ and 5+, consistent with a symmetric distribution of charge (Figure 1A), while the monomers from the disulfide-reduced BLG show dominant 7+ and 4+ charge states, which are more asymmetric (Figure 1C). This result corresponds to what was observed by Jurchen et al. for α-lactalbumin.[18,19] Parts A and C of Figure 2 show that at lower CID energies (<800 eV) both oxidized and reduced precursors yield primarily charge-symmetric monomers. However, at higher CID energies, asymmetric charge distributions result, with the disulfide-reduced sample producing a greater percentage of monomers with an asymmetric monomer charge distribution relative to the oxidized sample. This indicates that higher CID energies promote restructuring/unfolding and charge migration; e.g., the energized protein subunit becomes more flexible.

https://doi.org/10.1021/jasms.3c00142
J. Am. Soc. Mass Spectrom. XXXX, XXX, XXX−XXX

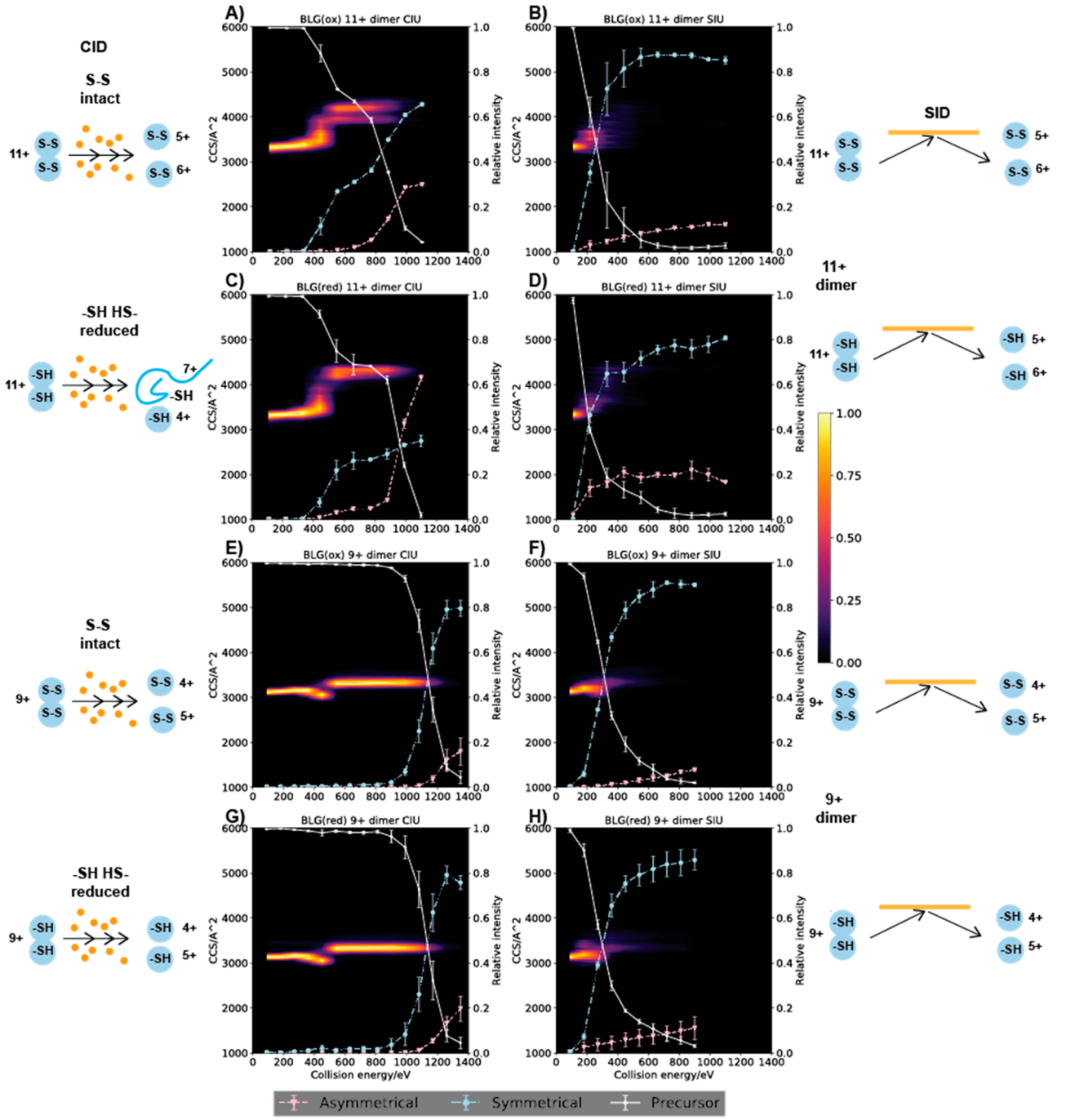

Figure 2. Unfolding profiles and overlaid energy-resolved mass spectra (ERMS) plots of the remaining precursor 11+ (A–D) /9+ (E–H) BLG dimer upon CID (left four) and SID (right four). Subfigures ABEF are from BLG with disulfide bonds intact (BLG(ox)), and CDGH are from the disulfide bond reduced (BLG(red)). Lines in the ERMS plots represent the relative intensities of different species versus the collision energies; white, remaining dimer precursor; pink, asymmetric charge partitioning monomers; light blue, symmetric charge partitioning monomers. Cartoons at the sides represent the dominant products at high energies (above 1,000 eV).

In contrast to the CID behavior, the SID shows different behaviors for the BLG dimers. When an SID energy of 550 eV is applied, the products have a charge-state distribution centered around 6+ and 5+. Values of 72% of 6+ and 5+ monomers in reduced dimers and 87% in oxidized dimers are observed, and the charge-state distribution is predominantly symmetric regardless of whether the disulfide bond is reduced or intact (Figure 1B,D). Interestingly, from SID, the reduced 11+ BLG dimer shows increasing, but still minor, 18% 7+ and 4+ monomer signals compared with the 8% in oxidized 11+ BLG dimer (Figure 2B,D). This could suggest that during the SID process there is a competition between charge migration and dissociation, with a fraction of the complexes following the unfolding/charge migration pathway. Alternatively, there could be some CID contamination in the experiments (gas is present in the SID region) or there could be a population of more than one initial structure impacting the surface (e.g., either the partial reduction did not reduce the same disulfide bond in all copies of the complex or a population of structures (including

https://doi.org/10.1021/jasms.3c00142
J. Am. Soc. Mass Spectrom. XXXX, XXX, XXX−XXX

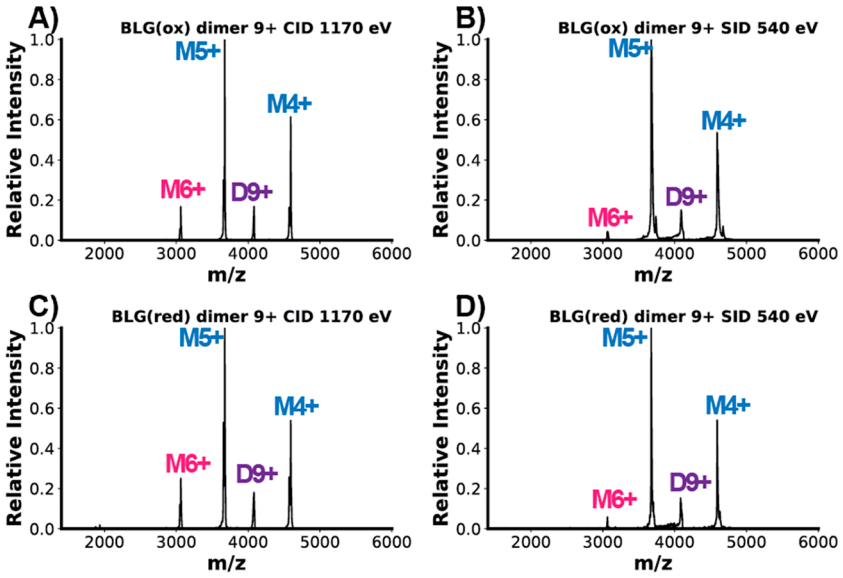

Figure 3. MSMS spectra of the 9+ BLG dimer. (A) CID 1170 eV of BLG dimer with disulfide bonds intact (BLG(ox)); (B) SID 540 eV of BLG(ox) dimer; (C) CID 1170 eV of BLG dimer with disulfide bond reduced (BLG(red)); (D) SID 540 eV of BLG(red) dimer. Blue and pink labels indicate charge symmetrically and asymmetrically distributed monomers, respectively; purple labels indicate precursor peaks, 'M' indicates monomer, 'D' indicates dimer, and the number indicates the charge state.

different protonated forms) is produced during ionization and transmission).

The combined results for the disulfide-reduced BLG suggest that the increase in flexibility within each subunit upon reduction does not influence the SID process as much as the CID process. The difference between the CID and SID behavior reveals different dominant dissociation pathways following the energy deposition process, with multistep activation in CID resulting in more unfolding and asymmetric charge distribution and the energy-jump activation in SID resulting in direct monomer−monomer separation.

The same dissociation trends recorded for BLG were also observed for the four-disulfide-containing protein α-lactalbumin (ALB). As shown in Figure S4, ALB(ox) shows a dominant symmetric charge distribution from both CID and SID throughout the energy range, whereas ALB(red) 11+ shows a dominant asymmetric charge distribution from CID. Similarly to BLG, when the precursor charge state is reduced, all conditions (CID or SID) generate monomers with symmetric charge partitioning. We also observed that ALB (red) had more precursor left than ALB(ox) for both CID and SID (Figure S4). A similar trend was also seen from BLG (Figure 1), but it is more pronounced with ALB. The increased remaining precursor abundance possibly suggests that increased flexibility requires energy for restructuring and/or leads to the production of a restructured (gas-phase annealed) form of the complex that is more difficult to dissociate.

Charge Reduction Changes the Restructuring and Results in Symmetric Charge Distributions by CID and SID. As shown in previous research, the reduction of precursor charge states will result in different dissociation pathways for CID processes.[21,22] It has also been suggested that lower charge states can preserve more native-like structures for proteins and protein complexes and stabilize them in the gas phase for many globular proteins and complexes.[21,23,23,36,41−43] In this work on β-lactoglobulin and α-lactalbumin, we further illustrate how the precursor charge states also play a role in the symmetry of the charge partitioning during the dissociation processes in CID and SID.

When we spray the homodimer β-lactoglobulin with 20% (v/v) TEAA (a charge-reducing agent), the charge-state distributions of the reduced and oxidized BLG dimers are similar and the 9+ dimers are the dominant dimer species (Figure S1C,D). The reduced and oxidized 9+ BLG have similar CCS values, which are 100 Å smaller than the 11+ dimers and closer to the theoretical CCS (Figure S3). Interestingly, when a charge reduced 9+ dimer precursor is selected, the charge-state distribution of products for either CID or SID through all the dissociation energies are the same for dimers with oxidized and reduced disulfide bonds. The 5+ and 4+ monomers are the dominant species (Figure 3) regardless of the oxidation state of the 9+ precursor.

CIU Reveals That an Unfolding Pathway Causes the Asymmetric Charge Partitioning. Collision-induced unfolding (CIU) profiles are widely used for the analysis of proteins and protein complexes, e.g., differentiating stability for protein variants, protein complexes, and antibodies.[20,35,44−49] CIU is used here to illustrate the relationship between asymmetric charge partitioning and the unfolding process. As shown in Figure 2A, the 11+ BLG dimer precursor keeps its original CCS when the CID energy is below 330 eV. From the overlaid energy-resolved mass spectrum (ERMS) plot, the precursor is intact in this low energy range as well. With increasing collision energy from 440 to 550 eV, the precursor experiences a dramatic structural change and undergoes dissociation. When the activation energy is higher than 550 eV, the CCS values of oxidized BLG dimer increase from approximately 3300 $Å^2$ in the native-like measurement to approximately 3900 and 4200 $Å^2$. However, the reduced BLG shows more extended conformations, with CCS around 4300 $Å^2$, at high collision energies, as expected by the release of one disulfide bond. There is also slightly more precursor preserved for reduced BLG (compared with BLG (ox)) with CID energies from 550 to 880 eV, which is likely because a greater fraction of the total energy is used to further unfold the

https://doi.org/10.1021/jasms.3c00142
J. Am. Soc. Mass Spectrom. XXXX, XXX, XXX−XXX

precursor and enhance the charge migration process. An alternative or additional explanation could be that the different rearranged/annealed structures require different dissociation energies. When the deposited collision energy is high enough (880 eV), the reduced BLG reaches its most extended conformation of 4310 Å^2. Production of monomers with complementary asymmetric charge partitioning (including 7+ and 4+ and 8+ and 3+) starts at around the same energy, which is consistent with the extension/restructuring of the precursor. These results indicate that the reduction of the disulfide bond increases the flexibility of the protein, and with high enough collision energy, the protein will start unfolding/restructuring, undergo further charge migration, and produce the asymmetric charge partitioning products.

The data presented in Figure 2 show that the symmetric monomer charge distribution at lower collision energies occurs with limited CCS change and the asymmetric charge distribution at higher collision energy occurs with unfolding, as evidenced by increasing CCS values. Our explanation is that CID is a multiple collision restructuring process. During CID, the collisions initiate some restructuring of the protein complex followed by and facilitating the charge migration. The proton migration could be driven by Coulombic repulsion,[50] salt bridge cleavages,[51,52] and local change in basicity[53] due to the structural changes. Charge migrations would enhance the unfolding and restructuring of the subunit. With unfolding and restructuring, the protein interface is disrupted as well. The restructured subunit will be ejected from the complex.[54] Thus, the process results in the asymmetric charge partitioning of the dissociated monomers.

In contrast to the CID behavior, the SID process deposits higher energy into the protein complex with only approximately a single collision step with a more massive target.[55] The large excess of internal energy[56] enables a kinetically favored dissociation process. This fast energy transfer is unlike the multiple-step CID energy deposition, limiting the multiple-step local restructuring process and allowing the disruption of interfacial interactions. The direct dissociation without large CCS changes in SID reveals the more "native-like" structure and topology of the protein complex and generates a more symmetric charge partitioning in the products. This mechanism is supported by the results shown in Figure 2B,D. The SIU plots show that the precursors are dissociated even at 220 eV SID energy and only a very small percentage of precursor remains around energies 220−440 eV, with more limited CCS change compared with the CIU plots in Figure 2A,C. From the ERMS plot in the SID data (Figure 2 B,D), we find that the charge distribution is still influenced by the reduction of the disulfide bond with more 7+ and 4+ monomers (20% at 660 eV) compared with the oxidized BLG (9% at 660 eV), although the 6+/5+ pair still dominates. The extended reduced dimer precursor has a CCS around 3800 Å^2, and oxidized BLG dimer precursor is around 3600 Å^2 at 330 eV. The observation of more 7+ and 4+ monomers with reduced dimer is also consistent with the observation of the more extended conformation of precursor left in the SIU of the reduced precursor at 330 eV.

An interesting result is apparent when the CCS profiles of the generated monomers are compared (Figure S5). The main characteristic that determines the CCS of the products is the charge state.[23] Most monomers produced from BLG share similar CCS at the same charge state regardless of the energy, precursor charge state, type of excitation, and number of disulfide bonds. The monomers are more compact (1750−1800 Å) at low (4−5) charge states and more extended (1900−2300 Å) at higher (6+ to ∼7+) charge states. As shown in Figure S3, the theoretical CCS of monomer is around 1650 Å and the experimental 5+ monomer CCS is around 1700 Å. One major difference appears for the SID 6+ monomers, which show two distinct conformations after dissociation. For all SID 6+ monomers, the more compact conformation, which has a CCS similar to that of the 6+ monomer from CID, is generated around 50 eV lower in energy than the extended conformation. One plausible explanation is that at lower SID energies, all of the energy is used for dissociation. At higher energies, the extra internal energy distributed into the complex is also used for restructuring;[57] however, this expansion does not involve charge migration because the CCS increase of 7+ monomers is very minor at high energy. Because the more extended 6+ conformer is produced at higher energies than the compact one and no significant increase in the higher charge product (e.g., 7+) is detected, we assume that the more extended product is the result of unfolding after activation or that two different charge distributions or two different disulfide reduction sites of dimer have different energy requirements for dissociation and unfolding. Formation of the 7+/4+ monomer pair from 11+ dimer is only a minor process for SID but is more significant and energy dependent for CID.

We next sought to determine the role of the precursor charge state in unfolding during the CIU and SIU processes. To do so, we selected a BLG complex with a lower charge state (+9) for the CIU and SIU experiments. When dimers with lower charge (+9 compared to +11) are selected for CID, both reduced and oxidized BLG samples produce monomers with remarkably similar, predominantly symmetric charge distributions. From both CIU plots (Figure 2E,G), the extended conformation of the 9+ dimer precursor has a CCS of around 3120 Å^2, which is much smaller than the 3900−4310 Å^2 expanded 11+ charge state. With limited structural expansion, the charge migration is limited and results in a symmetric charge distribution of the products. Note that the dimer precursor undergoes compaction prior to an abrupt, but limited, expansion in the CID 400−500 eV range. Collision-induced dissociation happens at significantly higher energies than the rearrangement of the 9+ precursor complex structure and requires a much higher CID energy compared with the 11+ precursor.

To further measure characteristics of the CID-restructured form of the 9+ dimer precursor, we performed SID on the in-source CID activated[24] 9+ dimeric precursor with disulfide bonds intact (Figure 4). The results show that with 200 V in-source cone activation the dimer is more extended/source-restructured, as shown by a shifted/later drift time distribution (Figure 4A). The in-source (CID) restructured 9+ dimer requires a significantly higher SID energy to dissociate than the original 9+ dimer and generates more monomers with charge asymmetrically distributed compared to the more native-like dimer that did not undergo restructuring in the source (Figure 4B,C). This suggests that the source-restructured (CID-restructured) dimer no longer preserves its entire, original native-like protein−protein interface; while some features of the original interface might still be intact, others may be lost and new interactions may have formed to produce the measured elongation and additional stability. Both the 9+ and 11+ precursor dimers undergo restructuring upon activation prior to dissociation. The extended conformation

https://doi.org/10.1021/jasms.3c00142
J. Am. Soc. Mass Spectrom. XXXX, XXX, XXX−XXX

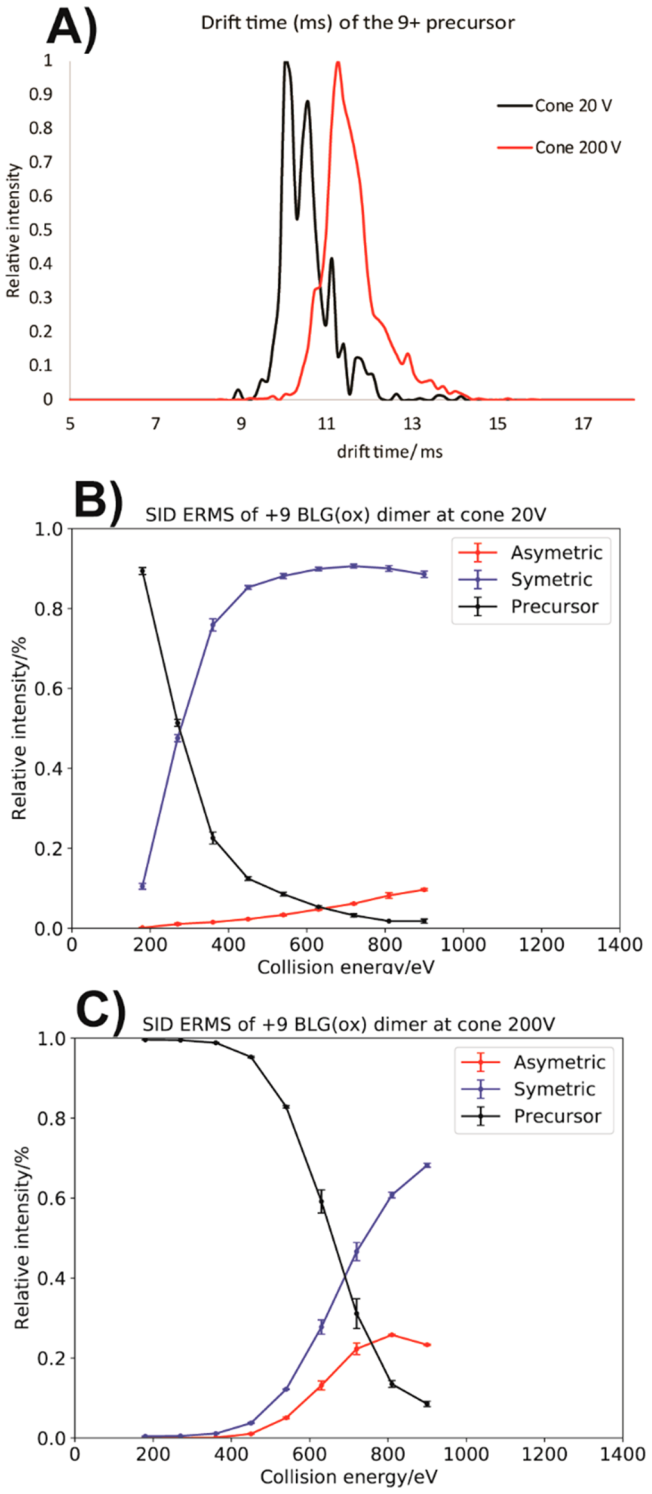

Figure 4. A) Drift time distributions of the 9+ BLG dimer with disulfide bonds intact, at cone voltages of 20 V (black) and 200 V (red). B) SID energy-resolved tandem mass spectra (ERMS) of the 9+ BLG (ox) dimer at cone voltage 20 V. C) SID energy-resolved tandem mass spectra of the 9+ BLG (ox) dimer at cone voltage 200 V. Black lines represent the relative intensity of the precursor, the red lines indicate the monomer products with an asymmetric charge distribution, and the blue lines indicate the monomer products with a symmetric charge distribution.

at 9+, e.g., in Figure 2E/G, has a smaller CCS compared to that of the extended 11+ dimer, e.g., in Figure 2 A/C, and CID generates a more symmetric charge-state distribution of the monomers for both oxidized and reduced 9+ dimeric protein.[23]

In the case of SIU, the charge-state distributions of the monomers are consistent with the precursor conformations measured by IM as well. The plots for oxidized versus reduced +9 BLG precursor (Figure 2F,H) are similar to each other; however, the disulfide bond reduced BLG has an extended conformation around 3500 Å^2 at SID energy 180−270 eV that is absent, or much less abundant, in the oxidized sample. Additionally, the ERMS plot for the reduced 9+ precursor shows slightly higher asymmetric 6+ and 3+ monomer products in addition to the dominant symmetric 5+ and 4+ monomers, consistent with greater flexibility offered by disulfide bond reduction.

The shapes of the ERMS plots for the precursor ions also supply clues about the protein structural differences and dissociation pathway differences. For CID, the reduction of precursor charge state results in a significant increase of dissociation onset energy (dissociation of 20% precursor) from 450 eV for 11+ to 1100 eV for 9+ precursor (Figure 2A,E). This large increase indicates that the number of charges plays a significant role in the dissociation process. Comparing the plots for +11 dimers with intact and reduced disulfide bonds (Figure 2A,C), the flatter slope in the 400−900 eV range indicates more energy is used in the restructuring process rather than the dissociation process after disulfide bonds are reduced. These experimental data are consistent with our computational model that showed that SID appearance energies can be predicted from structural features of the protein−protein interface, including intrasubunit rigidity.[36,58]

In contrast to CIU and ERMS plots, the SIU and ERMS plots of the 9+ and 11+ precursor dimers (Figure 2B−H) share similar features. The reduction of the charge state only increases the onset from around 150 to 200 eV, which is much smaller than the CID onset energy increase (450−1100 eV). Moreover, the reduction of the disulfide does not dramatically change the shape of the precursor SID ERMS plot, although the SIU plot for 9+ shows a minor shift in CCS at the lowest SID energy that causes dissociation (180 eV). This suggests that the major SID process does not involve significant structural change and the dissociation is more dependent on the initial, not restructured, interfaces of the protein complexes. From previous research, SID onset energy is correlated to the interfacial size/strength of the protein complexes.[36,58] The small difference in the ERMS onset energy (lowest energy where dissociation is measurable) for 9+ vs 11+ BLG dimers suggests the preservation of a similar interface at different charge states. Overall, the results are consistent with SID dissociating/measuring "native-like" interfaces. The similar CCS values of the monomeric product ions, regardless of the activation energy or activation type, suggest that the monomeric product ions have enough energy to reach a stable gas-phase structure prior to the CCS measurement.

Competition between Dissociation and Unfolding Pathways. The results presented here suggest that competition between direct dissociation and restructuring of the protein complexes occurs with CID and SID. With the disulfide bonds intact, the BLG has a more rigid structure and a relatively small interface (468 Å^2, from Proteins, Interfaces, Structures, and Assemblies (PISA) analysis[59] of PDB 2Q2M), consistent with a high energy barrier for unfolding and charge migration compared with dissociation. In this case, both the

https://doi.org/10.1021/jasms.3c00142
J. Am. Soc. Mass Spectrom. XXXX, XXX, XXX−XXX

CID and SID lead to monomer products without charge migration. Unfolding/restructuring can occur for both the oxidized and reduced forms of the dimer, although the barriers and extent of unfolding will differ. In the unfolding pathway, the energy barrier is determined by the structures. With gradual restructuring from multiple collisions in CID, charge migration is promoted, decreasing the energy barrier for further restructuring.[53,60,61] During the restructuring process, the interfacial interactions are gradually disrupted and finally lead to the ejection of the unfolding monomer.[53] Moreover, when at least one disulfide bond is reduced, the energy barrier of the further unfolding process is predicted to be lower than that for the protein complex with all disulfide bonds intact. The charge partitioning of the CID monomers is similar in the 400−900 eV range for the 11+ dimer, however, as illustrated in Figure 2C; the 4+ and 7+ monomer pair from the disulfide-reduced dimer starts increasing more dramatically as a function of collision energy when the energy is higher than 900 eV (Figure 2A,C). When only one disulfide bond is reduced, the energy barrier for charge migration is still slightly higher than the dissociation energy barrier. Therefore, there is a competition between the two pathways. When the CID energy is not high enough for significant restructuring, the dimer undergoes the dissociation pathway to produce the charge symmetric 5+ and 6+ monomer pairs as the dominant products. The increasing dissociation energy overcomes the charge migration energy barrier to a more extended conformation, which results in a charge migration pathway for the CID process with an asymmetric charge distribution.

Unlike CID, SID of the dimers does not suggest a multicollisional restructuring/unfolding process followed by dissociation from the unfolded state for the majority of the dimer population. Rather, the restructuring and dissociation happen at the same stage after an "energy-jump" deposition, with the majority of the dimer population dissociating and the remainder (minor population) restructuring (Figure 2B,D). From the SIU, the remaining precursor is unfolded to a similar extent as it is in CID. More symmetric charge partitioning is observed in SID suggesting that most of the deposited energy is used for dissociation rather than restructuring, prior to dissociation. (see decrease of the precursor in the ERMS plots, Figure 2B,D,F,G). The proposed mechanism for SID is that the large energy deposition and redistribution of the internal energy leads to a more kinetically favored fast dissociation pathway without restructuring and charge migration, producing a symmetric (native-like) charge distribution.[62]

When the number of charges on the protein complex decreases, the number of ways to arrange those charges into structures without significant Coulombic repulsion is increased. This reduces the extent of restructuring and charge migration of the complex. As a result, the 9+ BLG dimer undergoes dissociation without a charge migration pathway over the measured energy range. This does not mean, however, that the 9+ dimer has not restructured because the 9+ dimer activated by in-source CID is much more difficult to fragment (requires a higher input of energy) by CID or SID than the initial 9+ dimer, while also producing different ratios of symmetrically to asymmetrically charged monomer products.

CONCLUSIONS

This work provides insights into the dissociation and restructuring pathways of homodimeric proteins with CID vs SID. The results confirm that the basis of the asymmetric charge partitioning in CID is the restructuring of the protein complex and that this restructuring process is less dominant with SID. Generally, SID exhibits reduced conformational disruptions (restructuring) of subunits prior to dissociation due to its ability to directly overcome the dissociation energy barrier, reducing the charge migration that occurs prior to dissociation. In contrast, CID favors restructuring pathways of the protein complexes, and this process is precursor charge-state dependent, with different structures produced for different precursor charge states. Use of both CID and SID for different charge-state precursors is recommended when characterizing the structure of an unknown protein complex to generate complementary structural information. CID and CIU are suggested when comparing flexibility or local structural change, while SID can be applied to interpret the native structure of the protein complexes. Further investigation with the same experimental design using heterodimers would increase our understanding of charge partitioning mechanisms in the protein complexes during dissociation. A final takeaway message, which reaffirms what we and others have cautioned in some settings, is that while CID of lower charge states can lead to symmetric charge partitioning, users should not assume that the dissociation has occurred from a native-like state; multistep CID activation can cause restructuring that precedes dissociation. This caution applies to in-source CID and in-source trapping that are often used to provide "cleaner" looking peaks. Practitioners should be aware that "pretty is not always better" if the goal is to fragment the native-like structure. Use in-source CID and in-source trapping with appropriate caution; they are useful for mass measurements but can cause problems for structure or stability determinations.

ASSOCIATED CONTENT

Supporting Information

The Supporting Information is available free of charge at https://pubs.acs.org/doi/10.1021/jasms.3c00142.

Mass spectra of the β-lactoglobulin dimers; collision cross-section of the β-lactoglobulin dimer and monomer; collision-induced dissociation and surface-induced dissociation spectra of α-lactalbumin 11+ dimer; collision-induced unfolding plots of the β-lactoglobulin monomers generated from dimers; detailed tuning parameters for the surface-induced dissociation device (PDF)

AUTHOR INFORMATION

Corresponding Author

Vicki H. Wysocki − *The Department of Chemistry and Biochemistry and Resource for Native Mass Spectrometry Guided Structural Biology, The Ohio State University, Columbus, Ohio 43210, United States;* orcid.org/0000-0003-0495-2538; Email: wysocki.11@osu.edu

Authors

Mengxuan Jia − *The Department of Chemistry and Biochemistry and Resource for Native Mass Spectrometry Guided Structural Biology, The Ohio State University, Columbus, Ohio 43210, United States;* orcid.org/0000-0001-9173-1084

https://doi.org/10.1021/jasms.3c00142
J. Am. Soc. Mass Spectrom. XXXX, XXX, XXX−XXX

Yang Song − *The Department of Chemistry and Biochemistry, The Ohio State University, Columbus, Ohio 43210, United States*

Chen Du − *The Department of Chemistry and Biochemistry and Resource for Native Mass Spectrometry Guided Structural Biology, The Ohio State University, Columbus, Ohio 43210, United States*

Complete contact information is available at: https://pubs.acs.org/10.1021/jasms.3c00142

Notes

The authors declare no competing financial interest.

■ ACKNOWLEDGMENTS

We are grateful for the financial support from the National Institutes of Health (Grants R01 GM113658 and P41GM128577 to V.H.W.). This work was inspired by previous related research of Evan Williams and co-workers; we are pleased to have it included in the virtual special focus issue honoring Evan's ASMS 2022 John B. Fenn Award for Distinguished Contribution in Mass Spectrometry.

■ REFERENCES

(1) Leney, A. C.; Heck, A. J. R. Native Mass Spectrometry: What Is in the Name? *J. Am. Soc. Mass Spectrom.* **2017**, *28* (1), 5−13.

(2) Robinson, C. V. Mass Spectrometry: From Plasma Proteins to Mitochondrial Membranes. *Proc. Natl. Acad. Sci. U.S.A.* **2019**, *116* (8), 2814−2820.

(3) Hopper, J. T. S.; Robinson, C. V. Mass Spectrometry of Intact Protein Complexes. *Proteomics for Biological Discovery*; John Wiley & Sons, Ltd, 2019; pp 145−173. DOI: 10.1002/9781119081661.ch6.

(4) Grandori, R. Origin of the Conformation Dependence of Protein Charge-State Distributions in Electrospray Ionization Mass Spectrometry. *J. Mass Spectrom.* **2003**, *38* (1), 11−15.

(5) Ruotolo, B. T. Evidence for Macromolecular Protein Rings in the Absence of Bulk Water. *Science* **2005**, *310* (5754), 1658−1661.

(6) Light-Wahl, K. J.; Schwartz, B. L.; Smith, R. D. Observation of the Noncovalent Quaternary Associations of Proteins by Electrospray Ionization Mass Spectrometry. *J. Am. Chem. Soc.* **1994**, *116* (12), 5271−5278.

(7) Benesch, J. L. P. Collisional Activation of Protein Complexes: Picking up the Pieces. *J. Am. Soc. Mass Spectrom.* **2009**, *20* (3), 341−348.

(8) Zhou, M.; Wysocki, V. H. Surface Induced Dissociation: Dissecting Noncovalent Protein Complexes in the Gas Phase. *Acc. Chem. Res.* **2014**, *47* (4), 1010−1018.

(9) Stiving, A. Q.; VanAernum, Z. L.; Busch, F.; Harvey, S. R.; Sarni, S. H.; Wysocki, V. H. Surface-Induced Dissociation: An Effective Method for Characterization of Protein Quaternary Structure. *Anal. Chem.* **2019**, *91* (1), 190−209.

(10) Jennings, K. R. The Changing Impact of the Collision-Induced Decomposition of Ions on Mass Spectrometry. *Int. J. Mass Spectrom.* **2000**, *200* (1), 479−493.

(11) Hall, Z.; Hernández, H.; Marsh, J. A.; Teichmann, S. A.; Robinson, C. V. The Role of Salt Bridges, Charge Density, and Subunit Flexibility in Determining Disassembly Routes of Protein Complexes. *Structure* **2013**, *21* (8), 1325−1337.

(12) Zhou, M.; Dagan, S.; Wysocki, V. H. Protein Subunits Released by Surface Collisions of Noncovalent Complexes: Nativelike Compact Structures Revealed by Ion Mobility Mass Spectrometry. *Angew. Chem., Int. Ed. Engl.* **2012**, *51* (18), 4336−4339.

(13) Song, Y.; Nelp, M. T.; Bandarian, V.; Wysocki, V. H. Refining the Structural Model of a Heterohexameric Protein Complex: Surface Induced Dissociation and Ion Mobility Provide Key Connectivity and Topology Information. *ACS Cent Sci.* **2015**, *1* (9), 477−487.

(14) Sahasrabuddhe, A.; Hsia, Y.; Busch, F.; Sheffler, W.; King, N. P.; Baker, D.; Wysocki, V. H. Confirmation of Intersubunit Connectivity and Topology of Designed Protein Complexes by Native MS. *Proc. Natl. Acad. Sci. U.S.A.* **2018**, *115* (6), 1268−1273.

(15) Busch, F.; VanAernum, Z. L.; Ju, Y.; Yan, J.; Gilbert, J. D.; Quintyn, R. S.; Bern, M.; Wysocki, V. H. Localization of Protein Complex Bound Ligands by Surface-Induced Dissociation High-Resolution Mass Spectrometry. *Anal. Chem.* **2018**, *90* (21), 12796−12801.

(16) Bush, M. F.; Hall, Z.; Giles, K.; Hoyes, J.; Robinson, C. V.; Ruotolo, B. T. Collision Cross Sections of Proteins and Their Complexes: A Calibration Framework and Database for Gas-Phase Structural Biology. *Anal. Chem.* **2010**, *82* (22), 9557−9565.

(17) Stiving, A. Q.; Jones, B. J.; Ujma, J.; Giles, K.; Wysocki, V. H. Collision Cross Sections of Charge-Reduced Proteins and Protein Complexes: A Database for Collision Cross Section Calibration. *Anal. Chem.* **2020**, *92* (6), 4475−4483.

(18) Jurchen, J. C.; Williams, E. R. Origin of Asymmetric Charge Partitioning in the Dissociation of Gas-Phase Protein Homodimers. *J. Am. Chem. Soc.* **2003**, *125* (9), 2817−2826.

(19) Jurchen, J. C.; Garcia, D. E.; Williams, E. R. Further Studies on the Origins of Asymmetric Charge Partitioning in Protein Homodimers. *J. Am. Soc. Mass Spectrom.* **2004**, *15* (10), 1408−1415.

(20) Hyung, S.-J.; Robinson, C. V.; Ruotolo, B. T. Gas-Phase Unfolding and Disassembly Reveals Stability Differences in Ligand-Bound Multiprotein Complexes. *Chemistry & Biology* **2009**, *16* (4), 382−390.

(21) Pagel, K.; Hyung, S.-J.; Ruotolo, B. T.; Robinson, C. V. Alternate Dissociation Pathways Identified in Charge-Reduced Protein Complex Ions. *Anal. Chem.* **2010**, *82* (12), 5363−5372.

(22) Hall, Z.; Politis, A.; Bush, M. F.; Smith, L. J.; Robinson, C. V. Charge-State Dependent Compaction and Dissociation of Protein Complexes: Insights from Ion Mobility and Molecular Dynamics. *J. Am. Chem. Soc.* **2012**, *134* (7), 3429−3438.

(23) Zhou, M.; Dagan, S.; Wysocki, V. H. Impact of Charge State on Gas-Phase Behaviors of Noncovalent Protein Complexes in Collision Induced Dissociation and Surface Induced Dissociation. *Analyst* **2013**, *138* (5), 1353.

(24) Quintyn, R. S.; Zhou, M.; Yan, J.; Wysocki, V. H. Surface-Induced Dissociation Mass Spectra as a Tool for Distinguishing Different Structural Forms of Gas-Phase Multimeric Protein Complexes. *Anal. Chem.* **2015**, *87* (23), 11879−11886.

(25) VanAernum, Z. L.; Gilbert, J. D.; Belov, M. E.; Makarov, A. A.; Horning, S. R.; Wysocki, V. H. Surface-Induced Dissociation of Noncovalent Protein Complexes in an Extended Mass Range Orbitrap Mass Spectrometer. *Anal. Chem.* **2019**, *91* (5), 3611−3618.

(26) VanAernum, Z.; Busch, F.; Jones, B. J.; Jia, M.; Chen, Z.; Boyken, S. E.; Sahasrabuddhe, A.; Baker, D.; Wysocki, V. Rapid Online Buffer Exchange: A Method for Screening of Proteins, Protein Complexes, and Cell Lysates by Native Mass Spectrometry. *ChemRxiv* **2019**, DOI: 10.26434/chemrxiv.8792177.v1.

(27) Marklund, E. G.; Degiacomi, M. T.; Robinson, C. V.; Baldwin, A. J.; Benesch, J. L. P. Collision Cross Sections for Structural Proteomics. *Structure* **2015**, *23* (4), 791−799.

(28) Bleiholder, C.; Wyttenbach, T.; Bowers, M. T. A Novel Projection Approximation Algorithm for the Fast and Accurate Computation of Molecular Collision Cross Sections (I). Method. *Int. J. Mass Spectrom.* **2011**, *308* (1), 1−10.

(29) Bleiholder, C.; Contreras, S.; Bowers, M. T. A Novel Projection Approximation Algorithm for the Fast and Accurate Computation of Molecular Collision Cross Sections (IV). Application to Polypeptides. *Int. J. Mass Spectrom.* **2013**, *354*−*355*, 275−280.

(30) Bleiholder, C.; Contreras, S.; Do, T. D.; Bowers, M. T. A Novel Projection Approximation Algorithm for the Fast and Accurate Computation of Molecular Collision Cross Sections (II). Model Parameterization and Definition of Empirical Shape Factors for Proteins. *Int. J. Mass Spectrom.* **2013**, *345*−*347*, 89−96.

(31) Anderson, S. E.; Bleiholder, C.; Brocker, E. R.; Stang, P. J.; Bowers, M. T. A Novel Projection Approximation Algorithm for the

Fast and Accurate Computation of Molecular Collision Cross Sections (III): Application to Supramolecular Coordination-Driven Assemblies with Complex Shapes. *Int. J. Mass Spectrom.* **2012**, *330–332*, 78–84.
(32) Benesch, J. L.; Ruotolo, B. T. Mass Spectrometry: Come of Age for Structural and Dynamical Biology. *Curr. Opin. Struct. Biol.* **2011**, *21* (5), 641–649.
(33) Ruotolo, B. T.; Benesch, J. L. P.; Sandercock, A. M.; Hyung, S.-J.; Robinson, C. V. Ion Mobility–Mass Spectrometry Analysis of Large Protein Complexes. *Nat. Protoc* **2008**, *3* (7), 1139–1152.
(34) Haynes, S. E.; Polasky, D. A.; Dixit, S. M.; Majmudar, J. D.; Neeson, K.; Ruotolo, B. T.; Martin, B. R. Variable-Velocity Traveling-Wave Ion Mobility Separation Enhancing Peak Capacity for Data-Independent Acquisition Proteomics. *Anal. Chem.* **2017**, *89* (11), 5669–5672.
(35) Eschweiler, J. D.; Rabuck-Gibbons, J. N.; Tian, Y.; Ruotolo, B. T. CIUSuite: A Quantitative Analysis Package for Collision Induced Unfolding Measurements of Gas-Phase Protein Ions. *Anal. Chem.* **2015**, *87* (22), 11516–11522.
(36) Harvey, S. R.; Seffernick, J. T.; Quintyn, R. S.; Song, Y.; Ju, Y.; Yan, J.; Sahasrabuddhe, A. N.; Norris, A.; Zhou, M.; Behrman, E. J.; Lindert, S.; Wysocki, V. H. Relative Interfacial Cleavage Energetics of Protein Complexes Revealed by Surface Collisions. *Proc. Natl. Acad. Sci. U. S. A.* **2019**, *116* (17), 8143–8148.
(37) Hoffmann, M. A. M.; van Mil, P. J. J. M. Heat-Induced Aggregation of β-Lactoglobulin: Role of the Free Thiol Group and Disulfide Bonds. *J. Agric. Food Chem.* **1997**, *45* (8), 2942–2948.
(38) Creamer, L. K.; Bienvenue, A.; Nilsson, H.; Paulsson, M.; van Wanroij, M.; Lowe, E. K.; Anema, S. G.; Boland, M. J.; Jiménez-Flores, R. Heat-Induced Redistribution of Disulfide Bonds in Milk Proteins. 1. Bovine β-Lactoglobulin. *J. Agric. Food Chem.* **2004**, *52* (25), 7660–7668.
(39) Cavanagh, J.; Benson, L. M.; Thompson, R.; Naylor, S. In Line Desalting Mass Spectrometry for the Study of Noncovalent Biological Complexes. *Anal. Chem.* **2003**, *75* (14), 3281–3286.
(40) Leonil, J.; Molle, D.; Fauquant, J.; Maubois, J. L.; Pearce, R. J.; Bouhallab, S. Characterization by Ionization Mass Spectrometry of Lactosyl β-Lactoglobulin Conjugates Formed During Heat Treatment of Milk and Whey and Identification of One Lactose-Binding Site. *Journal of Dairy Science* **1997**, *80* (10), 2270–2281.
(41) Ma, X.; Zhou, M.; Wysocki, V. H. Surface Induced Dissociation Yields Quaternary Substructure of Refractory Noncovalent Phosphorylase B and Glutamate Dehydrogenase Complexes. *J. Am. Soc. Mass Spectrom.* **2014**, *25* (3), 368–379.
(42) Zhong, Y.; Han, L.; Ruotolo, B. T. Collisional and Coulombic Unfolding of Gas-Phase Proteins: High Correlation to Their Domain Structures in Solution. *Angew. Chem., Int. Ed.* **2014**, *53* (35), 9209–9212.
(43) Sever, A. I. M.; Konermann, L. Gas Phase Protein Folding Triggered by Proton Stripping Generates Inside-Out Structures: A Molecular Dynamics Simulation Study. *J. Phys. Chem. B* **2020**, *124* (18), 3667–3677.
(44) Shelimov, K. B.; Clemmer, D. E.; Hudgins, R. R.; Jarrold, M. F. Protein Structure *in Vacuo*: Gas-Phase Conformations of BPTI and Cytochrome *c*. *J. Am. Chem. Soc.* **1997**, *119* (9), 2240–2248.
(45) Dixit, S. M.; Polasky, D. A.; Ruotolo, B. T. Collision Induced Unfolding of Isolated Proteins in the Gas Phase: Past, Present, and Future. *Curr. Opin. Chem. Biol.* **2018**, *42*, 93–100.
(46) Tian, Y.; Han, L.; Buckner, A. C.; Ruotolo, B. T. Collision Induced Unfolding of Intact Antibodies: Rapid Characterization of Disulfide Bonding Patterns, Glycosylation, and Structures. *Anal. Chem.* **2015**, *87* (22), 11509–11515.
(47) Gadkari, V. V.; Juliano, B. R.; Mallis, C. S.; May, J. C.; Kurulugama, R. T.; Fjeldsted, J. C.; McLean, J. A.; Russell, D. H.; Ruotolo, B. T. Performance Evaluation of In-Source Ion Activation Hardware for Collision-Induced Unfolding of Proteins and Protein Complexes on a Drift Tube Ion Mobility-Mass Spectrometer. *Analyst* **2023**, *148* (2), 391–401.
(48) Vallejo, D. D.; Kang, J.; Coghlan, J.; Ramírez, C. R.; Polasky, D. A.; Kurulugama, R. T.; Fjeldsted, J. C.; Schwendeman, A. A.; Ruotolo, B. T. Collision-Induced Unfolding Reveals Stability Differences in Infliximab Therapeutics under Native and Heat Stress Conditions. *Anal. Chem.* **2021**, *93* (48), 16166–16174.
(49) Nash, S.; Vachet, R. W. Gas-Phase Unfolding of Protein Complexes Distinguishes Conformational Isomers. *J. Am. Chem. Soc.* **2022**, *144* (48), 22128–22139.
(50) Mao, Y.; Ratner, M. A.; Jarrold, M. F. Molecular Dynamics Simulations of the Charge-Induced Unfolding and Refolding of Unsolvated Cytochrome *c*. *J. Phys. Chem. B* **1999**, *103* (45), 10017–10021.
(51) Loo, R. R. O.; Loo, J. A. Salt Bridge Rearrangement (SaBRe) Explains the Dissociation Behavior of Noncovalent Complexes. *J. Am. Soc. Mass Spectrom.* **2016**, *27* (6), 975–990.
(52) Schnier, P. D.; Gross, D. S.; Williams, E. R. Electrostatic Forces and Dielectric Polarizability of Multiply Protonated Gas-Phase Cytochrome c Ions Probed by Ion/Molecule Chemistry. *J. Am. Chem. Soc.* **1995**, *117* (25), 6747–6757.
(53) Popa, V.; Trecroce, D. A.; McAllister, R. G.; Konermann, L. Collision-Induced Dissociation of Electrosprayed Protein Complexes: An All-Atom Molecular Dynamics Model with Mobile Protons. *J. Phys. Chem. B* **2016**, *120* (23), 5114–5124.
(54) Fegan, S. K.; Thachuk, M. A Charge Moving Algorithm for Molecular Dynamics Simulations of Gas-Phase Proteins. *J. Chem. Theory Comput.* **2013**, *9* (6), 2531–2539.
(55) Anggara, K.; Ochner, H.; Szilagyi, S.; Malavolti, L.; Rauschenbach, S.; Kern, K. Landing Proteins on Graphene Trampoline Preserves Their Gas-Phase Folding on the Surface. *ACS Cent. Sci.* **2023**, *9* (2), 151–158.
(56) Vékey, K. Internal Energy Effects in Mass Spectrometry. *Journal of Mass Spectrometry* **1996**, *31* (5), 445–463.
(57) Donor, M. T.; Mroz, A. M.; Prell, J. S. Experimental and Theoretical Investigation of Overall Energy Deposition in Surface-Induced Unfolding of Protein Ions. *Chem. Sci.* **2019**, *10* (14), 4097–4106.
(58) Seffernick, J. T.; Harvey, S. R.; Wysocki, V. H.; Lindert, S. Predicting Protein Complex Structure from Surface-Induced Dissociation Mass Spectrometry Data. *ACS Cent. Sci.* **2019**, *5* (8), 1330–1341.
(59) Krissinel, E.; Henrick, K. Inference of Macromolecular Assemblies from Crystalline State. *J. Mol. Biol.* **2007**, *372* (3), 774–797.
(60) Ruotolo, B. T.; Hyung, S.-J.; Robinson, P. M.; Giles, K.; Bateman, R. H.; Robinson, C. V. Ion Mobility–Mass Spectrometry Reveals Long-Lived, Unfolded Intermediates in the Dissociation of Protein Complexes. *Angew. Chem., Int. Ed.* **2007**, *46* (42), 8001–8004.
(61) Felitsyn, N.; Kitova, E. N.; Klassen, J. S. Thermal Decomposition of a Gaseous Multiprotein Complex Studied by Blackbody Infrared Radiative Dissociation. Investigating the Origin of the Asymmetric Dissociation Behavior. *Anal. Chem.* **2001**, *73* (19), 4647–4661.
(62) Beardsley, R. L.; Jones, C. M.; Galhena, A. S.; Wysocki, V. H. Noncovalent Protein Tetramers and Pentamers with " *n* " Charges Yield Monomers with *n* /4 and *n* /5 Charges. *Anal. Chem.* **2009**, *81* (4), 1347–1356.

https://doi.org/10.1021/jasms.3c00142
J. Am. Soc. Mass Spectrom. XXXX, XXX, XXX–XXX